Method to Maintain Artificial Gravity during Transfer Maneuvers for Tethered Spacecraft

Damon F. Landau*

Purdue University, W. Lafayette, IN, 47907

Traditional methods of producing artificial gravity rely on thrusting through the center of mass of the spacecraft, which entails a crew cabin that is either large (in length) increasing mass, or tethered to the propellant tanks requiring reconfiguration during maneuvers. An alternative approach requires offset thrusting, but allows a mass-competitive crew cabin that provides artificial gravity during maneuvers without the need to reconfigure the spacecraft. The thrust direction is controlled by adjusting the spin rate as decreasing propellant mass perturbs the system. This method is applied to a round-trip mission to Mars with high thrust engines.

Nomenclature

$\mathbf{a}$	=	acceleration vector, m/s^2
a_{AG}	=	artificial gravity level, m/s^2
f	=	internal force, N
g	=	standard acceleration due to gravity, m/s^2
I_{sp}	=	specific impulse of thruster, s
l	=	tether length, m
M_P	=	propulsion system mass, kg
M_H	=	crew habitat mass, kg
M	=	total spacecraft mass, kg
$\dot{m}$	=	propellant flow rate, kg/s
R	=	reaction control force, N
$\mathbf{r}$	=	position vector, m
T	=	thrust, N
$\mathbf{v}$	=	velocity vector, m/s
ΔV	=	change in velocity for transfer maneuver, m/s
ϕ	=	spacecraft roll angle
θ	=	spacecraft orientation angle, deg.
Ω	=	spacecraft orientation angle, deg.
ψ	=	thruster offset angle, deg.

I. Introduction

Perhaps the most iconic vision of artificial gravity occurs in Stanley Kubrick's *2001: A Space Odyssey* when a Pan Am shuttle waltzes to "The Blue Danube" with a large toroidal space station. Such rigid, axisymmetric structures are convenient to transfer a crew about the solar system, as the main engines can simply thrust through the center of mass along the spin axis while the vehicle maintains artificial gravity (as in Figure 1a). The key drawback to these structures is that they must be relatively large in dimension to provide artificial gravity at reasonable spin rates, which often leads to prohibitive launch masses. Instead of rotating the entire vehicle, a short-arm centrifuge could be integrated into the crew cabin.[1] However, in this case, the artificial gravity is intermittent, the cabin design cannot take advantage of any gravity benefits, and accommodating the additional equipment increases cabin mass. An alternative is to design the crew cabin for minimum mass, tether it to the propellant tanks as a counterweight, and spin the system, producing artificial gravity (as in Figure 1b). (Using a different counterweight such as consumables, power system, or a lander could increase risk by distancing the crew from potential life support elements.) In this scenario the only additional mass compared to a mission without artificial gravity is the (comparatively diminutive) tether. Thrusting through the center of mass in this case requires either spinning down and reeling together the entire system (which turns off or possibly reverses gravity during the maneuver) as depicted

* Currently at Jet Propulsion Laboratory, California Institute of Technology, Pasadena, California 91109-8099 Engineer, Trajectory Design and Navigation, M/S 301-121, Member AIAA.

in Figure 2a, or constantly adjusting the tether to the center of mass as the tanks expend propellant as in Figure 2b.[2–6] A method that provides artificial gravity throughout a mission with a fixed tethered configuration involves thrusting askew to the center of mass. In this case (Figure 3) the thrusters essentially drag the crew module at an angle to the spin axis, and the resulting moment (from the product of inertia) is canceled by the moment of the thruster (created by the thrust offset). The orientation during maneuvers remains fixed relative to the spin axis and the entire burn occurs in the desired direction.

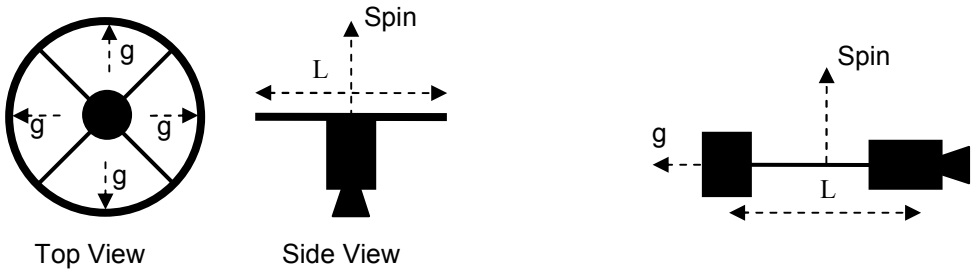

a) Spin length provided by cabin dimension. b) Spin length provided by tether or truss.

Figure 1 Potential spacecraft configurations to provide artificial gravity.

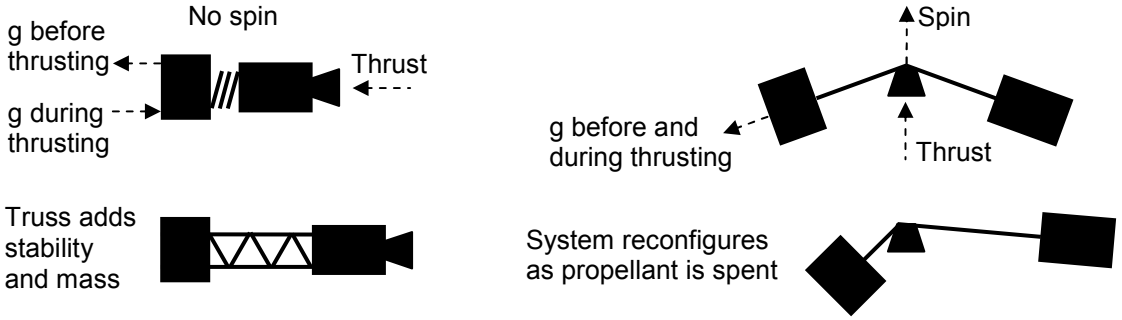

a) Gravity changes by spinning down to thrust. b) Configuration changes to thrust while spinning.

Figure 2 Thrusting through the center of mass presents issues for tethered systems.

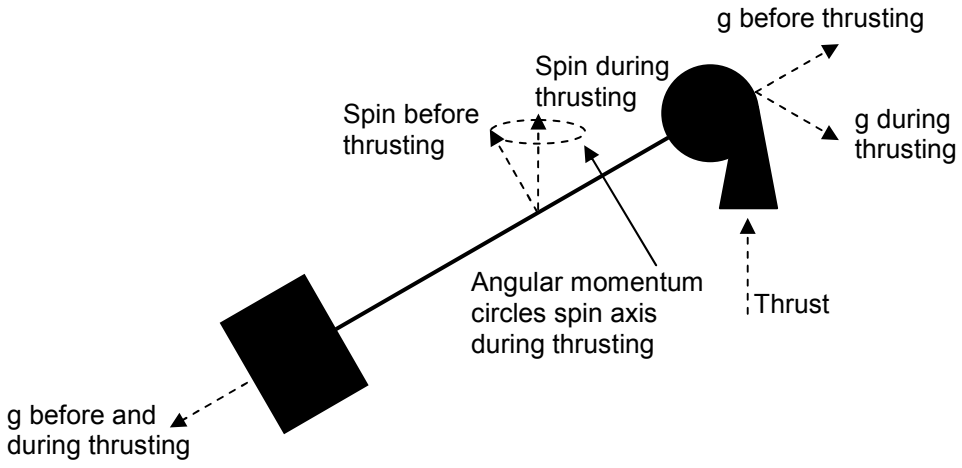

Figure 3 Gravity direction and system configuration do not change with offset thrusting.

II. Dynamics of thrusting, spinning system with variable mass

During a major transfer maneuver (e.g. injecting onto an interplanetary trajectory from Earth orbit) with a chemical system, the spacecraft experiences high accelerations (on the order of 1 g) and may expel more than half of its mass in propellant over several minutes. The effects of large torques (due to high thrust) and substantial changes

in mass distribution (due to high mass flow rates) can produce extreme variations in the orientation of the spacecraft during these critical maneuvers. (The dynamics for spacecraft with electric propulsion are the same, but are significantly more manageable due to the minute accelerations and mass flow rates and the extended operation times.) Because execution errors during transfer maneuvers translate into propellant mass growth and potential loss of the mission, the thrust vector must be controlled to the required direction. Moreover, the spacecraft design should be as robust and cost effective as possible, suggesting that a fixed configuration (with constant tether length and body-fixed thrust direction) would be prudent. The spacecraft design is further simplified by not requiring the crew cabin to contend with multiple acceleration directions (e.g. reversal of nominal gravity direction during maneuvers). Therefore a desirable design maintains artificial gravity with a fixed spacecraft configuration while allowing the thrust direction to be controlled during transfer maneuvers.

Figure 4 defines a body-fixed 3-2 rotation sequence for the orientation of the spacecraft. The propulsion system and crew habitat are modeled as point masses, so rotation about the $\hat{\mathbf{r}}$ axis is not dynamically significant. Moreover the tether is assumed to be massless and inelastic. The desired thrust direction is along $\hat{\mathbf{z}}$ so the control objective is to keep θ, which defines the tether offset from $\hat{\mathbf{z}}$, equal to ψ, which defines the thrust offset from the tether. For simplicity, the desired thrust direction is assumed to be inertially fixed. When $\theta = \psi$, the thrust is along $\hat{\mathbf{z}}$.

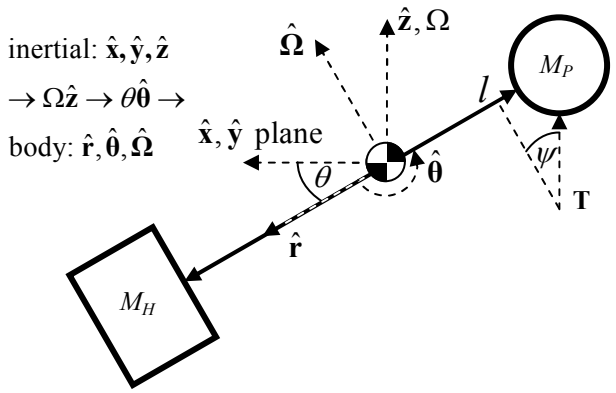

Figure 4 Definition of spacecraft orientation angles.

For the chosen rotation sequence the angular velocity is given by Eq. (1)

$$ {}^{x}\vec{\boldsymbol{\omega}}^{r} = -\dot{\Omega}\sin\theta\hat{\mathbf{r}} + \dot{\theta}\hat{\boldsymbol{\theta}} + \dot{\Omega}\cos\theta\hat{\boldsymbol{\Omega}} \tag{1} $$

Then, the kinematics of the habitat and propulsion system with respect to the center of mass are provided by Eq. (2) and Eq. (3), respectively.

$$ \begin{aligned} \mathbf{r}_H - \mathbf{r}_{CM} &= lM_P/M\,\hat{\mathbf{r}} \\ \mathbf{v}_H - \mathbf{v}_{CM} &= \left(l\dot{m}M_H/M^2\right)\hat{\mathbf{r}} + \left(lM_P/M\right)\dot{\Omega}\cos\theta\hat{\boldsymbol{\theta}} - \left(lM_P/M\right)\dot{\theta}\hat{\boldsymbol{\Omega}} \\ \mathbf{a}_H - \mathbf{a}_{CM} &= \left[-2l\dot{m}^2M_H/M^3 + l\ddot{m}M_H/M^2 - \left(lM_P/M\right)\left(\dot{\Omega}^2\cos^2\theta + \dot{\theta}^2\right)\right]\hat{\mathbf{r}} \\ &\quad + \left[\left(2l\dot{m}M_H/M^2\right)\dot{\Omega}\cos\theta + \left(lM_P/M\right)\left(\ddot{\Omega}\cos\theta - 2\dot{\Omega}\dot{\theta}\sin\theta\right)\right]\hat{\boldsymbol{\theta}} \\ &\quad + \left[-\left(2l\dot{m}M_H/M^2\right)\dot{\theta} - \left(lM_P/M\right)\left(\dot{\Omega}^2\cos\theta\sin\theta + \ddot{\theta}\right)\right]\hat{\boldsymbol{\Omega}} \end{aligned} \tag{2} $$

$$ \begin{aligned} \mathbf{r}_P - \mathbf{r}_{CM} &= -lM_H/M\,\hat{\mathbf{r}} \\ \mathbf{v}_P - \mathbf{v}_{CM} &= \left(l\dot{m}M_H/M^2\right)\hat{\mathbf{r}} - \left(lM_H/M\right)\dot{\Omega}\cos\theta\hat{\boldsymbol{\theta}} + \left(lM_H/M\right)\dot{\theta}\hat{\boldsymbol{\Omega}} \\ \mathbf{a}_P - \mathbf{a}_{CM} &= \left[-2l\dot{m}^2M_H/M^3 + l\ddot{m}M_H/M^2 + \left(lM_H/M\right)\left(\dot{\Omega}^2\cos^2\theta + \dot{\theta}^2\right)\right]\hat{\mathbf{r}} \\ &\quad + \left[\left(2l\dot{m}M_H/M^2\right)\dot{\Omega}\cos\theta - \left(lM_H/M\right)\left(\ddot{\Omega}\cos\theta - 2\dot{\Omega}\dot{\theta}\sin\theta\right)\right]\hat{\boldsymbol{\theta}} \\ &\quad + \left[-\left(2l\dot{m}M_H/M^2\right)\dot{\theta} + \left(lM_H/M\right)\left(\dot{\Omega}^2\cos\theta\sin\theta + \ddot{\theta}\right)\right]\hat{\boldsymbol{\Omega}} \end{aligned} \tag{3} $$

In these equations, variations in l are omitted because the tether length is assumed to be constant (for the fixed configuration system). A notable inclusion are variations in mass, where $\dot{m}$ is the mass flow rate (negative as

propellant is expelled from M_P). So, the thrust direction is assumed to be body fixed (ψ is constant), but the thrust magnitude may vary (i.e. the engines are throttleable). The motion of the center of mass depends on the motions of the habitat and propulsion system point masses according to Eq. (4). Again the variation of the propulsion system mass is taken into account.

$$\begin{aligned}\mathbf{r}_{cm} &= \left(M_H\mathbf{r}_H + M_P\mathbf{r}_P\right)/M \\ \mathbf{v}_{cm} &= \left[M_H\mathbf{v}_H + M_P\mathbf{v}_P + \dot{m}\left(\mathbf{r}_p - \mathbf{r}_{cm}\right)\right]/M \\ \mathbf{a}_{cm} &= \left[M_H\mathbf{a}_H + M_P\mathbf{a}_P + 2\dot{m}\left(\mathbf{v}_p - \mathbf{v}_{cm}\right) + \ddot{m}\left(\mathbf{r}_p - \mathbf{r}_{cm}\right)\right]/M\end{aligned} \tag{4}$$

Applying Newton's second law to the total system provides Eq. (5), where R is a reaction control force in the $\hat{\boldsymbol{\theta}}$ or $\hat{\boldsymbol{\Omega}}$ direction applied at either the habitat or propulsion system.

$$M_H\mathbf{a}_H + M_P\mathbf{a}_P = -T\sin\psi\hat{\mathbf{r}} + \left(R_{\theta H} + R_{\theta P}\right)\hat{\boldsymbol{\theta}} + \left(T\cos\psi + R_{\Omega H} + R_{\Omega P}\right)\hat{\boldsymbol{\Omega}} \tag{5}$$

The motion of the center of mass in inertial space is then provided by Eq. (6), where Eq. (3)–Eq. (5) are combined with the direction cosine matrix for the rotation sequence depicted in Figure 4.

$$\mathbf{a}_{cm} = \begin{bmatrix}\cos\Omega\cos\theta & -\sin\Omega & \cos\Omega\sin\theta \\ \cos\Omega\sin\theta & \cos\Omega & \sin\Omega\sin\theta \\ -\sin\theta & 0 & \cos\theta\end{bmatrix}\begin{bmatrix}-T\sin\psi/M + 2l\dot{m}^2M_H/M^3 - l\ddot{m}M_H/M^2 \\ \left(R_{\theta H} + R_{\theta P}\right)/M - \left(2l\dot{m}M_H/M^2\right)\dot{\Omega}\cos\theta \\ T\cos\psi/M + \left(R_{\Omega H} + R_{\Omega P}\right)/M + \left(2l\dot{m}M_H/M^2\right)\dot{\theta}\end{bmatrix} \tag{6}$$

Newton's second law is now applied to the habitat mass by combining Eq. (2) with Eq. (6) (in body coordinates), providing Eq. (7) where the accelerations (bracketed terms) are separated by coordinates. Similarly, the forces and accelerations for the propulsion system are provided in Eq. (8). The f terms in Eq. (7) and Eq. (8) are internal (tether) forces, where $f_{rH} = -f_{rP}$ is the tether tension and $f_{\theta H} = -f_{\theta P}$, $f_{\Omega H} = -f_{\Omega P}$ are transverse forces applied at the tether endpoints. These transverse forces would result in a net torque on the tether because they are opposite in sign and applied over a moment arm l. But the tether is assumed to be massless, so there can be no net torque and these forces must be zero $f_{\theta H} = f_{\theta P} = f_{\Omega H} = f_{\Omega P} = 0$.

$$\begin{aligned}\hat{\mathbf{r}}: \quad & f_{rH} = M_H\left[-T\sin\psi/M - \left(lM_P/M\right)\left(\dot{\Omega}^2\cos^2\theta + \dot{\theta}^2\right)\right] \\ \hat{\boldsymbol{\theta}}: \quad & R_{\theta H} + f_{\theta H} = M_H\left[\left(R_{\theta H} + R_{\theta P}\right)/M + \left(lM_P/M\right)\left(\ddot{\Omega}\cos\theta - 2\dot{\Omega}\dot{\theta}\sin\theta\right)\right] \\ \hat{\boldsymbol{\Omega}}: \quad & R_{\Omega H} + f_{\Omega H} = M_H\left[T\cos\psi/M + \left(R_{\Omega H} + R_{\Omega P}\right)/M - \left(lM_P/M\right)\left(\dot{\Omega}^2\cos\theta\sin\theta + \ddot{\theta}\right)\right]\end{aligned} \tag{7}$$

$$\begin{aligned}\hat{\mathbf{r}}: \quad & -T\sin\psi + f_{rP} = M_P\left[-T\sin\psi/M + \left(lM_H/M\right)\left(\dot{\Omega}^2\cos^2\theta + \dot{\theta}^2\right)\right] \\ \hat{\boldsymbol{\theta}}: \quad & R_{\theta P} + f_{\theta P} = M_P\left[\left(R_{\theta H} + R_{\theta P}\right)/M - \left(lM_H/M\right)\left(\ddot{\Omega}\cos\theta - 2\dot{\Omega}\dot{\theta}\sin\theta\right)\right] \\ \hat{\boldsymbol{\Omega}}: \quad & T\cos\psi + R_{\Omega P} + f_{\Omega P} = M_P\left[T\cos\psi/M + \left(R_{\Omega H} + R_{\Omega P}\right)/M + \left(lM_H/M\right)\left(\dot{\Omega}^2\cos\theta\sin\theta + \ddot{\theta}\right)\right]\end{aligned} \tag{8}$$

The $\hat{\boldsymbol{\theta}}$ and $\hat{\boldsymbol{\Omega}}$ components in Eq. (7) provide the rotational equations of motion for the system.

$$\begin{aligned}\ddot{\Omega} &= 2\dot{\Omega}\dot{\theta}\tan\theta + \left(R_{\theta H}M_P - R_{\theta P}M_H\right)/\left(lM_HM_P\cos\theta\right) \\ \ddot{\theta} &= -\dot{\Omega}^2\cos\theta\sin\theta + T\cos\psi/lM_p - \left(R_{\Omega H}M_P - R_{\Omega P}M_H\right)/lM_HM_P\end{aligned} \tag{9}$$

An interesting characteristic of these equations is that the decreasing moment of inertia due to propellant loss does not affect the rotational motion of the system. As pointed out by Belknap,[7] the motion of the lost mass once it leaves the spacecraft nullifies effects of the decreasing spacecraft inertia. Essentially any mass that leaves the spacecraft with zero relative velocity at the point of departure does not affect the angular velocity of the spacecraft; instead, it can affect the translational motion according to Eq. (4). Any mass that departs with non-zero relative velocity is modeled as thrust according to Eq. (10).

$$T = -\dot{m}gI_{sp} \tag{10}$$

The condition that permits $\theta = \psi$, and points the thrust along $\hat{\mathbf{z}}$, is found by setting $\ddot{\theta} = 0$ in Eq. (9) to arrive at Eq. (11). A key result of this equation is that the changing propulsion system mass M_P perturbs the orientation of the thrusting spacecraft. As propellant is lost, either the thrust must decrease or the spin rate must increase to

balance the system at $\theta = \psi$. Variations in l or ψ would also help balance the system, but require a reconfigurable spacecraft.

$$T \big/ \dot{\Omega}^2 = M_p l \sin\psi \tag{11}$$

Eq. (11) can be differentiated to produce Eq. (12), which provides a control law for the spin rate. The desired change in spin rate is then substituted into Eq. (9) to solve for the reaction force required to track Eq. (11). As indicated by Eq. (13), when the engine is throttled ($\ddot{m}$) to balance the mass loss ($\dot{m}$), no reaction forces are required. Any time that the engine is throttled at a different rate (or kept at constant thrust), the spin rate may be adjusted by thrusting along $\hat{\boldsymbol{\theta}}$ to maintain $\theta = \psi$. From Eq. (9), reaction thrust along $\hat{\boldsymbol{\Omega}}$ could also maintain thrust is the desired direction, but requires magnitudes on the same order as the main thruster T. Alternatively, the spin rate may be adjusted with relatively little thrust, providing an efficient pointing method.

$$\ddot{\Omega} = -\left(\ddot{m} g I_{sp} + \dot{\Omega}^2 \dot{m} l \sin\psi\right) \big/ 2\dot{\Omega} M_p l \sin\psi \tag{12}$$

$$R_{\theta H} M_P - R_{\theta P} M_H = -\left(\ddot{m} g I_{sp} + \dot{\Omega}^2 \dot{m} l \sin\psi\right) M_H \big/ 2\dot{\Omega} \tan\psi \tag{13}$$

Thus far, it has been assumed that the thruster is always pointed opposite of $\hat{\mathbf{z}}$ to maximize the amount of thrust in the desired direction. However, a slight roll along $\hat{\mathbf{r}}$ would point a fraction of the main thrust along $\hat{\boldsymbol{\theta}}$, effectively providing a reaction force. Moreover, this reaction force can track a nonlinear control input by adjusting the roll angle to any desired value. Thus the reaction force applied at the propulsion system end $R_{\theta P}$ in Eq. (13) may be replaced with the component of thrust in the $\hat{\boldsymbol{\theta}}$ direction $T \cos\psi \sin\phi$, where ϕ is the roll angle along $\hat{\mathbf{r}}$, resulting in Eq. (14).

$$\sin\phi = -\left(\ddot{m} g I_{sp} + \dot{\Omega}^2 \dot{m} l \sin\psi\right) \big/ 2\dot{m} g I_{sp} \dot{\Omega} \sin\psi \tag{14}$$

When the spacecraft is rolled to point thrust along $\hat{\boldsymbol{\theta}}$, the component of thrust along the main thrust direction $\hat{\boldsymbol{\Omega}}$ is decremented by $1 - \cos\phi$ and the component along $\hat{\mathbf{r}}$ remains $T \sin\psi$. But for small angles, the loss of thrust along $\hat{\boldsymbol{\Omega}}$ is very small (on the order of $T\phi^2$), so the component that adjusts spin rate is achieved essentially for free. Thus, Eq. (14) may be used to maintain the condition in Eq. (11) that allows a spacecraft to thrust in a desired direction while spinning to maintain artificial gravity. The translational motion of the system is governed by Eq. (6), and the rotational dynamics are given by Eq. (9).

III. Application to a round trip mission to Mars

A stop-over mission architecture[8] is assumed for the analysis. This mission type begins with the interplanetary transfer vehicle in a long period, elliptical orbit around Earth. The crew rendezvous with the transfer vehicle by taking a smaller "taxi" vehicle from the surface to the same orbit as the transfer vehicle. Then, the crew, taxi, and transfer vehicle depart Earth for a several-month journey to Mars. Upon approaching Mars, the crew departs the transfer vehicle in the taxi and go directly to the surface. The transfer vehicle propulsively captures into another long period elliptical orbit and remains in orbit during the stay time at Mars. (The crew and taxi are not necessarily with the transfer vehicle during Mars orbit insertion.) At the conclusion of the surface stay, the crew again rendezvous with the transfer vehicle in Mars orbit via the taxi. Following another several-month journey, the crew lands on Earth in the taxi while the transfer vehicle propulsively captures into Earth orbit to await refurbishment for subsequent missions. Key design parameters are provided in Table 1.

Table 1 Mission design assumptions

Parameter	Value	Notes
Earth orbit capture or departure ΔV	1 km/s	Long period elliptical orbit. Moderate interplanetary V_{∞}.
Mars orbit capture or departure ΔV	1.5 km/s	Long period elliptical orbit. Moderate interplanetary V_{∞}.
Crew habitat mass	40 t	Crew of 6.
Engine I_{sp}	450 s	Liquid hydrogen/liquid oxygen.
Engine inert/propellant mass ratio	0.16	Cryogenic upper stage.
Propulsion system staging	After Mars orbit insertion	Earth-Mars stage expended at Mars. Mass optimal to split mission ΔV equally.
Engine throttle range	60–100%	Adds controllability. Limited range simplifies engine design.
Engine ramp up/ramp down	5 s	Time between zero thrust and full throttle.
Artificial gravity level	1 g at Earth 0.38 g at Mars	Vary linearly during interplanetary transit to acclimate crew.
Maximum spin rate	4 rpm	Avoid motion sickness.
Maximum acceleration	2 g	Limit stress to crew and tether tension.

The propulsion system is sized via the rocket equation. In Eq. (15), the payload for the Mars-Earth stage is the crew habitat, and the payload for the Earth-Mars stage is the habitat and Mars-Earth stage. The resulting vehicle masses are provided in Table 2, where M_P is the total mass of the propulsion system and $M_{\text{propellant}}$ is the propellant mass for a single maneuver. The 11.1 t of inert mass for the Earth-Mars stage is discarded after Mars orbit insertion.

$$M_P = M_{\text{payload}} \left\{ \frac{\exp\left(\Delta V / g I_{sp}\right)}{1 - \frac{\text{inert}}{\text{propellant}}\left[\exp\left(\Delta V / g I_{sp}\right) - 1\right]} - 1 \right\}$$
$$M_{\text{propellant}} = M\left[1 - \exp\left(-\Delta V / g I_{sp}\right)\right] \tag{15}$$

Table 2 Vehicle mass at major events

Event	M, t	M_P, t	$M_{\text{propellant}}$, t	M_{inert}, t
Earth departure	161	121	32.6	
Mars arrival	128	88.4	37.0	11.1
Mars departure	80.3	40.3	23.1	
Earth arrival	57.1	17.1	11.6	5.5

The artificial gravity level sensed by the crew when the spacecraft is not thrusting is given by Eq. (16). From Table 2 the value for M_P/M is the smallest at Earth arrival, making this event the design driver for tether length. For a maximum angular velocity of 4 rpm, the tether length must be at least 187 m to provide 1 g of artificial gravity at Earth arrival. A 200 m tether is selected to provide margin.

$$a_{AG} = \omega^2 l\, M_P / M \tag{16}$$

The maximum acceleration limit is used to size the thrust level, which, as indicated by Eq. (11), also sets the body fixed thrust angle ψ. The largest acceleration on the spacecraft is likely to occur at Earth arrival because the artificial gravity component begins at 1 g, and the additional thrust continually increases this value as the burn progresses. (The spacecraft could be spun down slightly to reduce the acceleration level, but additional propellant would be required.) However, the crew is not on the spacecraft for this maneuver (they are landing in the taxi

vehicle), so the Earth departure maneuver becomes the event where the crew senses the highest acceleration. From Eq. (7) the sensed acceleration while thrusting is calculated with Eq. (17), where it is noted that $\theta = \psi, \dot{\theta} = 0$ during the maneuver. Moreover, the artificial gravity level when the thrust cuts off is set to be 1 g, which affects the design according to Eq. (18). [Eq. (18) equals Eq. (17) when $\theta = \psi, T = \dot{\theta} = 0$.] These two equations combine with Eq. (11) to uniquely solve for T, ψ, and Ω at the end of the Earth departure burn (where from Table 2 , M_p = 121 – 32.6 = 88.4 t). For a maximum limit of 2 g, the resulting values are T = 1.78 MN, ψ = 45 deg., and $\dot{\Omega}$ =3.60 rpm. A similar procedure could be used to design T and ψ for a maximum acceleration on the Earth arrival maneuver, except Eq. (18) would be applied to the beginning of the burn while Eq. (17) still applies to the end of the burn.

$$a_{\text{thrusting}} = T \sin\psi / M + \left(lM_P / M\right)\left(\dot{\Omega}^2 \cos^2\theta + \dot{\theta}^2\right) \tag{17}$$

$$a_{AG} = \left(lM_P / M\right)\left(\dot{\Omega}^2 \cos^2\psi\right) \tag{18}$$

If the engines were completely throttleable (from 0–100%), then the spacecraft design would be complete as the thrust level could be adjusted to match any combination of spin rate and mass according to Eq. (11). However, many engines do not operate at low throttle levels, so a throttle range of 60–100% is imposed. The method is still applicable for engines with limited throttle range by adjusting the spin rate before maneuvers; however, the large difference in spacecraft mass from beginning to end of the mission suggest that smaller (or fewer) engines should be used for the Mars-Earth stage. The engines are sized based on the rotation rates required for the artificial gravity level just before or after a maneuver, so that additional propellant is not spent adjusting the spin rate. The spin rates for artificial gravity from Eq. (18) and associated thrust values from Eq. (11) are provided in Table 3. The spin rate during thrusting $\dot{\Omega}$ is higher than the rate with free motion because the spacecraft is forced to rotate about a shorter radius (by a factor of $\cos\psi$) due to thrust. The thrust levels for Mars arrival and Earth arrival are both about half of the Earth departure thrust, while the Mars departure thrust is about 1/6$^{\text{th}}$ of the Earth departure value. Accounting for 60% throttle levels, a single 500 kN could be designed with four engines used at Earth departure, 2 engines at Mars arrival and Earth arrival, and a single engine at Mars departure. In this way, cost is reduced by requiring only one main engine to be built and qualified.

Table 3 Thrust design points

Event	a_{AG}, g	$\dot{\Omega}$, rpm	T, kN
End of Earth departure	1	3.60	1,781
Beginning of Mars arrival	0.38	2.22	677
End of Mars departure	0.38	3.37	301
Beginning of Earth arrival	1	5.46	793

After Mars orbit insertion, the Earth-Mars inert mass is expended by simply releasing the stage. By releasing the stage, no change in angular velocity in imparted to the spacecraft, but it does acquire a ΔV of a few m/s. To avoid additional thrusting that adjusts the spin rate before Mars departure, the thrust at the end of Mars arrival and the thrust at the beginning of Mars departure are throttled so that the respective angular velocities are equal. [Thrust affects spin rate via Eq. (11).] After arrival at Earth, a new 120-t propulsion stage replaces the 5.5-t inert Mars-Earth mass by docking at the center of mass and crawling out to the end of the tether. No external torques are applied and all mass transfer occurs at the center of mass, so angular momentum is conserved during this process resulting in a $\dfrac{M_{P0}/M_0}{M_{Pf}/M_f} = \dfrac{5.5/45.5}{121/161} = 0.160$ reduction in angular velocity. Thus, the engines are throttled to maximize the angular velocity at the end of the Earth arrival burn and the throttle at Earth departure is set to minimize angular velocity in order to reduce the change in spin rate that the reaction control thrusters must impart before the Earth departure maneuver. The final design consideration that is addressed is engine start and cutoff times. For example, a spacecraft that spins at a rate of 4 rpm makes a complete revolution every 15 seconds, and the thruster is aligned in the desired direction for only an instant each during each revolution. If the thrusters require even a few seconds to ramp up to full throttle, the impulse imparted during ramp up will be in an undesirable direction, resulting in a ΔV misalignment. To account for these effects, a five second interval between zero thrust

and full throttle is assumed, with a linear change in thrust level over the interval. The set of mission design parameters are compiled in Table 4.

Table 4 Derived spacecraft parameters

Parameter	Value
Tether length	200 m
Engine thrust	500 kN
# of Earth departure engines	4
# of Mars arrival engines	2
# of Mars departure engines	1
# of Earth arrival engines	2
Thruster offset angle	45 deg.

IV. Results

The spacecraft performance during the four main maneuvers is depicted in Figure 5–Figure 10. The throttle level at the beginning and end of the maneuvers is adjusted to provide a desired spin rate (e.g. spin to produce 1 g of artificial gravity at Earth departure). The thrust level is varied linearly during the maneuver, and the maneuver time is adjusted until the component of ΔV along $\hat{\mathbf{z}}$ is equal to the desired value. The initial conditions are derived by beginning with the desired state [Eq. (11)] and propagating the 5-s ramp-up time backwards. These derived initial conditions ensure that full thrust begins when $\theta = \psi$. From the initial state, the translational motion is modeled via Eq. (6), the rotational motions follows Eq. (9), and the control command is calculated using Eq. (14).

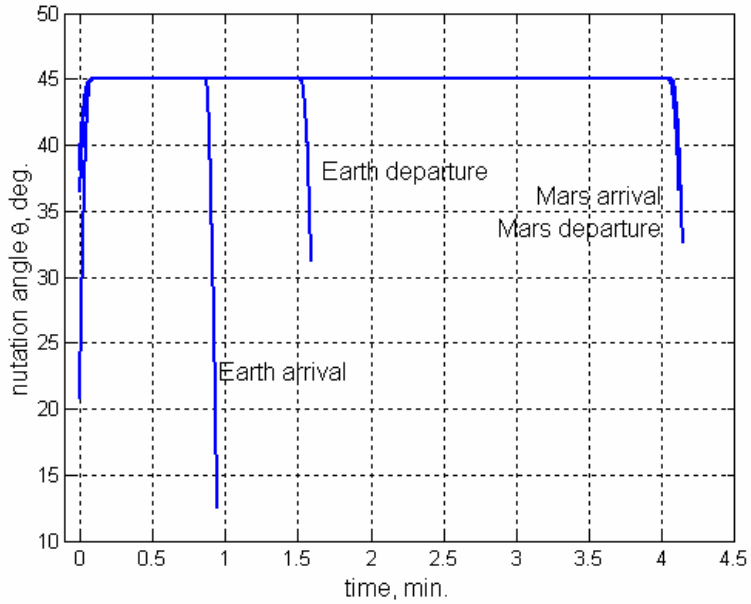

Figure 5 Thrust direction angle during four transfer maneuvers.

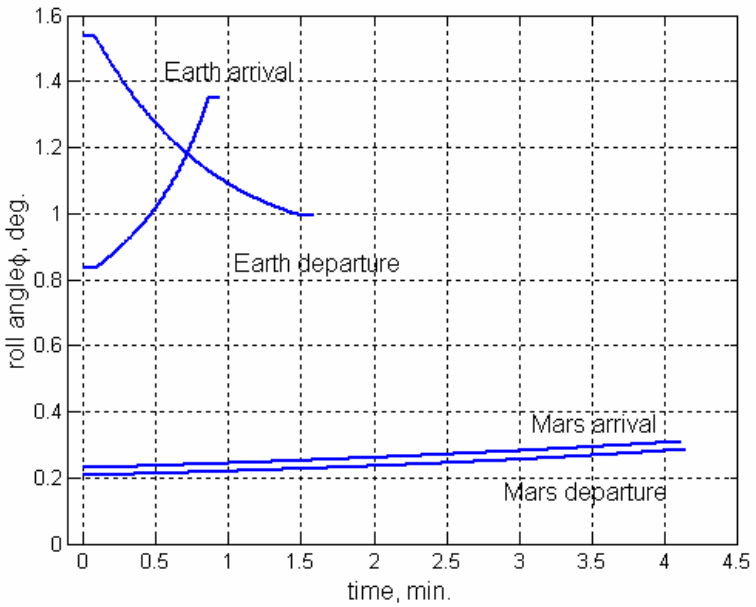

Figure 6 Thrust direction control during four transfer maneuvers.

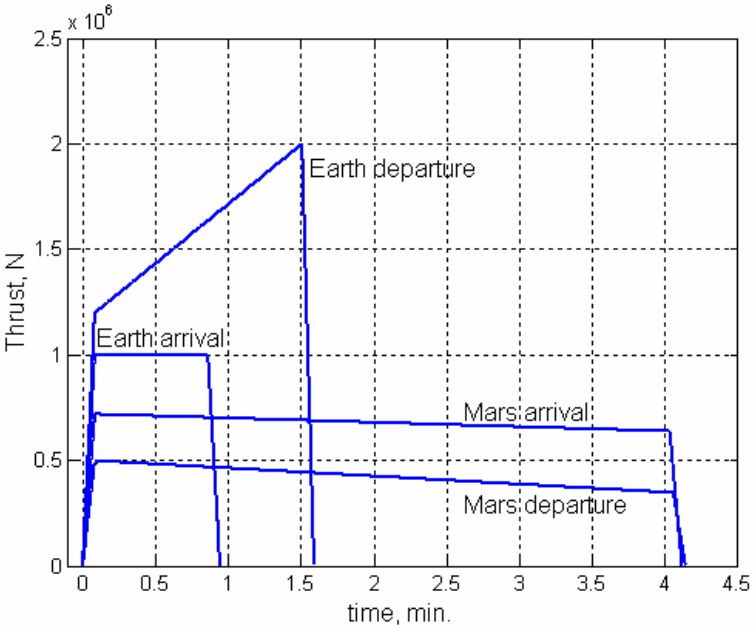

Figure 7 Thrust magnitude during four transfer maneuvers.

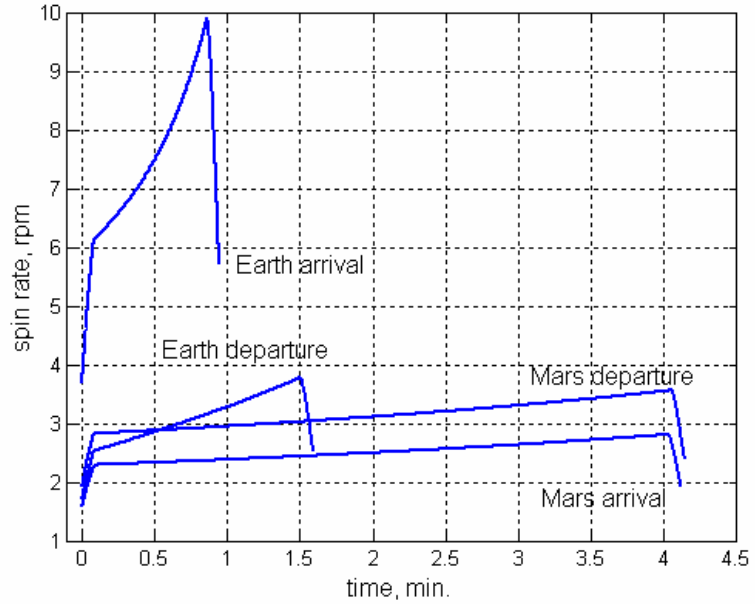

Figure 8 Spacecraft spin rate during four transfer maneuvers.

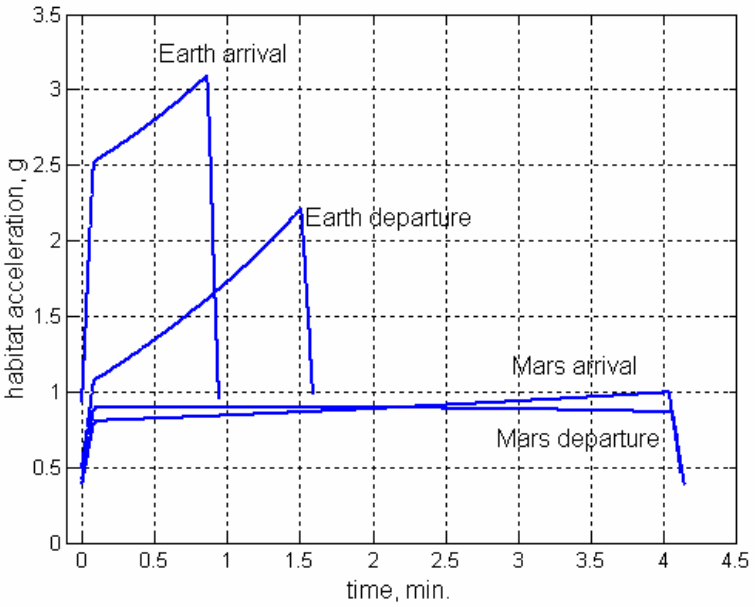

Figure 9 Acceleration of crew habitat during four transfer maneuvers.

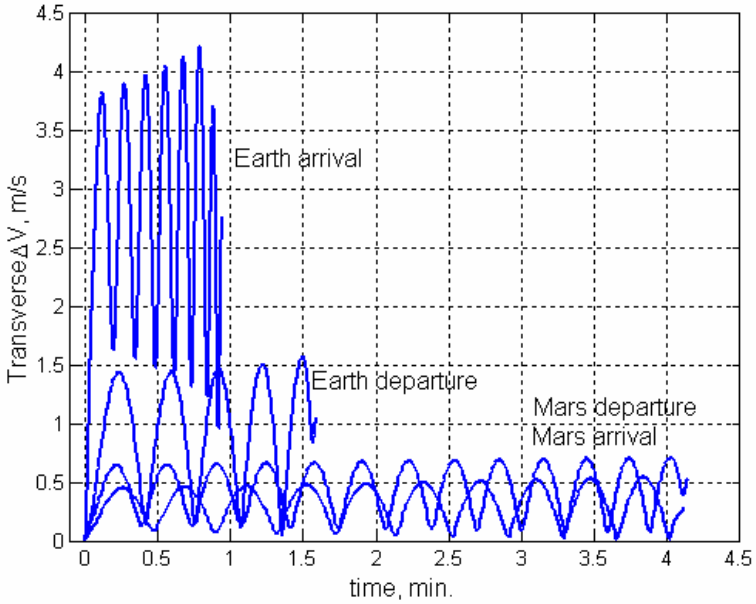

Figure 10 ΔV error during four transfer maneuvers.

In Figure 5, the thrust direction tracks the 45 deg. requirement while the thrusters are at their operational throttle levels. During the 5-s ramp up and ramp down times before and after the maneuvers the spacecraft transitions between free motion (θ oscillates as the spacecraft spins at an angle to $\hat{\mathbf{z}}$) and powered flight where θ is controlled. The spacecraft orientation is controlled by adjusting the thrust direction as demonstrated in Figure 6. The roll angle is around 1 deg. for maneuvers at Earth and less the 0.3 deg. at Mars. These small angles adjust the spin rate of the spacecraft to track Eq. (11) as the propellant mass depletes. The thrust profiles are shown in Figure 7, where the Earth departure stage has the largest throttle variation. The final thrust is maximized to achieve a final spin rate that provides 1-g artificial gravity [spin rate tracks thrust according to Eq. (11)]. The 5-s ramp up and ramp down periods are also visible in this figure. In Figure 8 the spin rates are moderate during all of the maneuvers except for Earth arrival. However in this case, the crew is not on board as they are landing on Earth in a taxi vehicle. The final spin rate is maximized because the rotation will drop considerably once a new propulsion system is added to the spacecraft (for the next mission to Mars). Specifically, the final spin rate of 5.7 rpm reduces to 0.9 rpm with the larger spacecraft. The required spin rate at the beginning of Earth departure is 1.7 rpm and additional propellant must be spent to increase the spin rate from the 0.9 rpm value. The high Earth arrival spin rate corresponds to a relatively large acceleration of 3 g in Figure 9. The tether mass would likely increase to accommodate the added tension, and this additional mass would trade against the propellant mass required to increase spin before Earth departure. If the tether mass needed to decrease, then the thrust at Earth arrival could throttle down. The design limit of 2 g is slightly exceeded at Earth departure; however, this is expected because the maximum thrust level (2 MN) is above the design level (1.8 MN). The Mars arrival and departure accelerations are at 0.38 g as specified in Table 1. The Earth arrival acceleration is slightly below 1 g, so some propellant is required to lower the spin rate to the maneuver value. If the initial thrust could be throttled to a slightly higher value, then the 1 g requirement can be met. Finally, the ΔV errors during the maneuver are given in Figure 10. The error is largest for Earth arrival mostly due to the poor thrust direction during the 5 seconds of ramp-up. Because the spin rate is high for this maneuver, the spacecraft thrusts over a large angle during the initial 5 seconds, which produces an transverse ΔV. The oscillations are large during this maneuver partly due to the comparatively large roll angle of 1 deg., which also produces ΔV in the plane normal to $\hat{\mathbf{z}}$. However, the spacecraft mass is small after this maneuver, so correction maneuvers require less propellant.

The propellant required to correct ΔV errors is combined with the additional propellant due to thrust offsets in Table 5. The "spin-up" column provides the propellant required when the spacecraft must completely spin down to perform transfer maneuvers, and gives a point of comparison to the present method, which allows the spacecraft to spin while thrusting. The spin up propellant is calculated via Eq. (19), which is derived by combining Eq. (16) and Eq. (9). This equation assumes that the spin up is effected by a thrust couple, which leads to the 2 coefficient.

$$M_{\text{propellant}} = 2\sqrt{a_{AG} l M_P / M}\left(M_H / g I_{sp}\right) \tag{19}$$

A specific impulse of 450 s is assumed for the spin up maneuver, which is probably high for a reaction control system. However, the thrust-while-spinning method still requires a thousand kg less propellant than the spin-down method. Moreover, most of the additional propellant is spent during the main maneuver, which uses the main engine with higher I_{sp}.

Table 5 Propellant mass comparison of spin down method and offset thrust method

Event	Spin up propellant, kg	Offset thrust propellant, kg
Earth departure	667	179
Mars arrival	411	125
Mars departure	272	87
Earth arrival	445	170
Total	1,795	750[a]

[a]Includes 189 kg to increase spin rate before Earth departure.

V. Conclusions

By judiciously balancing the thrust magnitude and spin rate, a spacecraft can perform large transfer maneuvers while spinning. For missions that employ artificial gravity, it is possible to complete the entire mission without having to despin the spacecraft and reel in a tether in order to perform a ΔV. A slight roll along the tether axis provides sufficient control to direct the thrust in a desired direction. Since the spacecraft never completely spins down, a significant amount of reaction control propellant is saved. A simpler spacecraft design may be available because artificial gravity as always present and the spacecraft configuration never has to change in order to complete the mission.

References

1. Kobric, R. L., Dara, S., Burley, J., and Gill S., "A new countermeasure device for long duration spaceflights," *Acta Astronautica*, Vol 58, No.10, 2006, pp. 523–536.
2. Clement, G. and Buckley A., *Artificial Gravity*, Microcosm, Hawthorn, CA, 2007.
3. Jokic, M. D. and Longuski, J. M., "Artificial Gravity and Abort Scenarios via Tethers for Human Missions to Mars," *Journal of Spacecraft and Rockets*, Vol. 42, No. 5, 2005, pp. 883–889.
4. Borowski, S. K., Dudzinski, L. A., and McGuire, M. L., "Artificial Gravity Vehicle Design Option for NASA's Human Mars Mission Using Bimodal NTR Propulsion," AIAA Paper 99-2545, June 1999.
5. McGuire, M. L., Borowski, S. K., Mason, L. M., and Gilland, J., "High Power MPD Nuclear Electric Propulsion (NEP) for Artificial Gravity HOPE Missions to Callisto," NASA TM-2003-212349, Washington, D.C., December 2003.
6. Benton, M. G. Sr., "Spaceship Discovery—Vehicle Architecture for Human Exploration of Moon, Mars, and Beyond," AIAA Paper 2006-7445, September 2006.
7. Belknap, S. A., "A General Transport Rule for Variable Mass Dynamics," *AIAA Journal,* Vol. 10, No. 9, 1972, pp. 1137–1138.
8. Niehoff, J., Friedlander, A., and McAdams, J., "Earth-Mars Transport Cycler Concepts," International Astronautical Federation, IAF Paper 91-438, International Astronautical Congress, Montreal, Canada, October 5–11, 1991.